

# Annealing Effects on the Crystallinity of Carbon Fiber-Reinforced Polyetheretherketone and Polyohenylene Laminate Composites Manufactured by Laser Automatic Tape Placement

Svetlana RISTESKA<sup>1\*</sup>, Anka TRAJKOVSKA PETKOSKA<sup>2</sup>, Samoil SAMAK<sup>3</sup>,  
Marian DRIENOVSKY<sup>4</sup>

<sup>1</sup> Institute for advance and composite and robotics, Krusevki pat, bb 7500 Prilep, Macedonia

<sup>2</sup> Faculty of Technology and Technical Sciences-Veles, University "St. Kliment Ohridski" – Bitola, Macedonia

<sup>3</sup> Mikrosam A.D., Krusevki pat, bb 7500 Prilep, Macedonia

<sup>4</sup> Faculty of Materials Science and Technology in Trnava, Slovak University of Technology, Jana Bottu 25, 917 24 Trnava, Slovakia

**crossref** <http://dx.doi.org/10.5755/j01.ms.26.3.21489>

Received 27 September 2018; accepted 01 March 2019

In situ consolidation of thermoplastic composites by Automated Tape Placement (ATP) is challenging. High quality ATP grade pre-preg material and tape head equipped with an efficient heat sources like lasers offer an opportunity towards high deposition rates and improved mechanical properties of composite materials. In this study uni-directional carbon fiber/polyphenylene sulfide (UD tape prepreg CF/PPS), carbon fiber/polyetheretherketone (UD tape prepreg CF/PEEK) as well as blend of carbon fiber/polyetheretherketone/polyphenylene sulfide (UD tapes prepreps CF/PEEK/PPS) laminates are compared in terms of their properties after beeing processed by ATP technology. CF/PPS, CF/PEEK and blend CF/PPS/PEEK laminate specimens were processed using in-situ laser-assisted ATP (LATP) process. LATP processing parameters used in this study were chosen based on a preliminary trials; the results provide a basis for refinement of these parameters and prepreg material with an optimal and balanced set of final mechanical properties. This study showed an attempt how to manage the processing parameters for LATP process and to obtain composite materials with tailored properties. The process for production of thermoplastic plates with LATP head in general is a process that is governed by many parameters such as: laser power, angle of incidence, roller pressure and temperature, placement speed, tool temperature, then types of the roller material and the tool material. These parameters are not subject of discussing in this paper; they are kept constant, and the goal of the paper is to manage the crystallinity level within the composite thermoplastic material during annealing step at different temperatures after LATP process. Also, the void content during the production process could be controlled. More particularly, the authors showed that composites based on PPS matrix manufactured with LATP process possess higher flexural strength, with less void content compared to samples based on PEEK matrix. These samples showed also higher crystallinity after annealing step.

**Keywords:** thermoplasts, laser-assisted automated tape placement (LATP), degree of crystallinity, void content, flexural strength.

## 1. INTRODUCTION

Thermoplastic composites are expected to undergo substantial growth over the next 10–20 years. The main advantages of thermoplastics compared to thermosetting composites are: rapid processing, reduced volatiles, improved reuse/recycle cycles, and in some cases reduced materials cost. These composites are attractive for application in the civil and military aerospace industry due to the high stiffness, fracture toughness, compressive strength, good impact, fatigue and chemical resistance properties. Another advantage of thermoplast composites is their ability to re-melt, which widens the possibilities in product and production process designs [1–5].

Thermoplastic tape placement is a special case of an out of autoclave process; it has high potential for aerospace industry due to its high degree of automation. Unidirectional (UD) continuous fiber reinforced tapes with high fiber content are used as semi-finished material. These tapes are

usually fully impregnated and consolidated with void content of approx. from 0.07 to 3.70 %. Within the thermoplastic tape placement process, tapes are melted by a heat source like, laser beam, infrared light, hot gas torch, and bonded to laminates by compaction force induced by a consolidation roller. During consolidation step, the tapes are cooled down to tool temperature (tool is made of Al alloys) [1, 2].

The recent advances in automated manufacturing technology of composite materials resulted in a highly promising process called fiber placement. The advantages of fiber-placement processes can be combined with the high throughputs that can be achieved using thermoplastic prepreg tape that can be shaped and consolidated online. This is enabled due to the chemical structure of the resin that melts under the heat regime and consolidation before the cooling step. Thus online consolidation technology has some advantages such as: i) eliminates the use of an autoclave by applying heat directly at the nip-point, ii)

\* Corresponding author. Tel.: ++389-70-353695; fax: ++389 (0)48 434 072. E-mail address: svetlanar@iacr.edu.mk (S. Risteska)

welding the tape on the preceding layer under compaction pressure, and iii) consolidating shortly behind the nip-point where the temperature is usually lower than in the previous step. Mechanisms governing strength buildup and consolidation during thermoplastic fiber-placement processes should be well understood in order to control the processing parameters to obtain the optimum product quality [3]. Laser-assisted tape placement was studied by many authors and described in literature [4–17]. Particularly, crystallization kinetics behavior of Polyetheretherketone (PEEK) based composites exposed to high heating and cooling rates is investigated by Tierney et. al., [16]. The rapid and appreciable crystal growth occurs under ultra-high heating and cooling rates.

Welding of semicrystalline thermoplastic UD tapes with LAMP (Laser-Assisted Tape-Placed) process is also analyzed in literature as well [6–10]. These studies have led researchers to measure the temperature distribution in the vicinity of the welded process zones [17–32]. The thermal history of the composite material during processing by LAMP is of great benefit to understand the bond quality and the properties that control e.g., crystallinity and void content in composite materials.

For different commercially available thermoplastic tapes it is very important to identify a LAMP process. The microstructure, bond strength measured by 3-point bending test (3-pbt) and degree of crystallinity of tested tapes at different temperatures are also presented. Good agreement between experimental and theoretical data was observed for examined samples.

## 2. EXPERIMENTAL DETAILS

### 2.1. Materials

The thermoplastic composite materials evaluated in this study are:

- LAMP1: UD prepreg material Suprem™ T with Carbon-fibre (Hexcel AS4 carbon fibre) and matrix PPS (Ticona 0214 PPS) supplied by Suprem™ (Switzerland);
- LAMP2: UD prepreg material Tenax®-E TPUD PEEK-HTS45 with Carbon-fibre (Tenax®-E HTS45 12K carbon fibre) and matrix PEEK (Vitrex 150 PEEK) supplied by Toho Tenax (Germany), and
- LAMP3: UD blended prepreg material Tenax®-E HTS45/150PEEK + Suprem™ T 60 % AS4/PPS-214 with 50/50 %.

**Table 1.** Description of UD prepreps (used in this study)

Materials	Tenax®-E TPUD HTS45/150PEEK	Suprem™ T 60% AS4/PPS-214
Prepreg areal weight	220 g/m <sup>2</sup>	305 g/m <sup>2</sup>
Fibre areal weight	145 g/m <sup>2</sup>	200 g/m <sup>2</sup>
Matrix content	34 wt. %	34 wt. %
Nominal thickness	0.14 mm	0.19 mm
Matrix glass transition temperature ( $T_g$ )	143 °C	80–90 °C
Matrix melting temperature ( $T_m$ )	342 °C	285 °C

All examined composite materials are summarized in Table 1. The tapes with 25.4 mm width were selected for LAMP process investigated in this work.

### 2.2. LAMP process (laser-assisted ATP manufacturing)

The LAMP process could be specified by a multitude of interdependent variables:

- LAMP operational parameters: laser energy density, angle of incidence, roller pressure (roller consolidation force), placement speed, tape placement track overlap from layer to layer, tool temperature and roller temperature;
- LAMP hardware parameters: roller material, tool material, and
- Prepreg properties: surface roughness, void content, initial crystallinity level, tape width.

A complex relationship exists between all of these variables and the resulting bond strength of composites. One of the most critical variable is the heat source and the resulting temperature distribution in the incoming tape and substrate, which strongly influences the resulting mechanical properties that could be „measured,“ through final void content as well as crystallinity level (in case of semi-crystalline thermoplastics such as: PEEK and PPS).

In this study, laminates were obtained by using a laser-assisted tape placement head (LAMP) manufactured by Mikrosam, Macedonia. LAMP head is attached to a robot arm (product by Kuka, KR 420 R3080), as it is shown in Fig. 1.

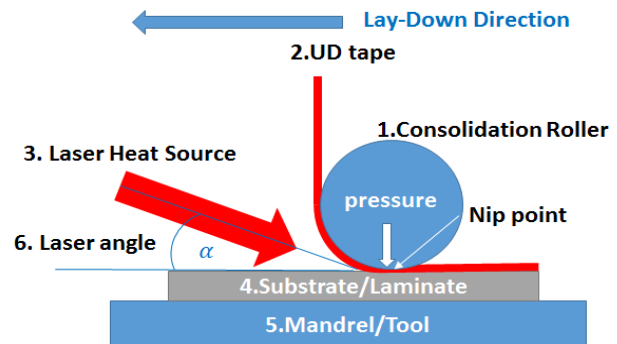


**Fig. 1.** A laser-assisted tape placement head (LAMP): 1–a consolidation roller (outer diameter of 90 mm); 2–a tape feed, guidance, tensioning, and cutting system for UD tape; 3–type -diode laser 3 kW, lens - type/focal length: array 2-LL-line 2.20; array 1-LL-line 2.10, spot dimension: laser beam width 28 mm and laser beam height 56 mm, focus: 250 mm by Laserline company; the heat source is focussed under angle  $\alpha$ ; 4–a substrate or laminate; 5–mandrel (tool) and a temperature sensor (pyrometer) that is built in the laser system

Flat panels (samples) were produced using LAMP head. The laser and pyrometer were set to operate in closed-loop control, i.e. the laser energy was controlled to minimize the error between the set point temperature and feedback temperature measurement from the pyrometer. All factors such as: type materials and process parameters for LAMP (laser energy density, tool temperature, consolidation force, laser angle of incidence, etc.) have a big influence on the interplay as well as on the void content inside the laminate

made by LAMP [17, 18]. In this study, the processing parameters (presented in Table 2) were chosen based on a number of trials performed by LAMP – head [17].

**Table 2.** Laser assisted ATP (LAMP) processing parameters used in the current study

Materials	LAMP1	LAMP2	LAMP3
Lay-up angle	[0] <sub>8</sub> *	[0] <sub>8</sub> *	[0] <sub>10</sub> *
Lay- down speed	9 m/min		
Target temperature	360 °C	420 °C	400 °C
Tool temperature	Unheated/no cooling		
Roller material	Rubber		
Tool material	Stainless steel		
angle of incidence	22.5°		
Roller pressure (consolidation f)	3.8 bar (365.56 N)		
*-numbers of layers			

## 2.3. Characterization of LAMP laminates

### 2.3.1. Optical microscopy characterization

The preparation and procedure for preparing the micrographic specimens of polymer composite materials in general is described elsewhere [33–37]. A sample was extracted from each plate of the LAMP laminates (LAMP1, LAMP2 and LAMP3), mounted in epoxy resin, grinded and adequately polished for further examination.

The image capture and analysis were performed and they were evaluated for the void content for each of the laminates manufactured by LAMP process. Segmentation of the fibres, resin and voids were performed on selected regions (10 images first method) using image analysis software Image J (NIH) [38].

The void content of composite product is very important parameter that characterizes the quality of the produced composite part. It was used also second method to characterize the quality of the produced part and it was calculated using the experimental and theoretical density of the composite according to Eq 1 [40]:

$$V_{void} = \frac{(\rho_{ct} - \rho_{ce})}{\rho_{ct}}, \quad (1)$$

where:  $V_{void}$  is void content of the composite;  $\rho_{ct}$  is theoretical density of the composite ( $\text{kg/m}^3$ );  $\rho_{ce}$  is experimental density of the composite ( $\text{kg/m}^3$ ). As stated above, method A from ASTM-D 792 standard was used to calculate the experimental density  $\rho_{ce}$  of the composite [40].

### 2.3.2. Mechanical tests

A three-point bending test was performed to measure the flexural mechanical properties of the composites according to ASTM D-790. Specimens with dimensions of 50.0 mm × 15.0 mm × 1.5 mm were tested at 5 mm/min crosshead speed and constant span at  $L = 16 \cdot d$  ( $d$  is thickness of the specimens). The composites produced only by LAMP usually show smaller values of flexural strength and stiffness compared to composites produced by autoclave process [27].

The flexural strength,  $\sigma_{max}$  can be determined by equations 2 and 3 [41]:

$$\sigma_{max} = \frac{3 F_{max} L}{2 b d^2}, \quad (2)$$

$$E_f = \frac{1}{4} \frac{L^3}{b d^3} \frac{\Delta F}{\Delta t}, \quad (3)$$

where:  $F$  is load at a given point on the load-deflection curve in N;  $b$  and  $d$  are the width and thickness of samples tested in mm, respectively;  $L$  is a support span in mm,  $E_f$  is the flexural modulus of elasticity given in MPa,  $\Delta t$  is difference in deflection between  $t_1$  and  $t_2$ ;  $\Delta F$  is difference in load;  $F_1$  and  $F_2$  at  $t_1$  and  $t_2$ , respectively [41].

### 2.3.3. Determination of degree of crystallinity of tested laminates

Differential scanning calorimetry (DSC, Netzsch model STA 409CD) was used to measure samples LAMP1, LAMP2 and LAMP3 in order to determine the degree of crystallinity of the tape after laser automatic tape placement at room temperature as well at different temperatures after annealing step.

The crystallinity of the welded tape (before and after the annealing step) was determined by heating samples from room temperature up to 600 °C with a heating rate of 10 °C/min. The tests were carried out under Ar atmosphere. The degree of the crystalline ( $X_c$ ) is calculate with Eq. 4 [29]:

$$X_c = \frac{|\Delta H_m| - |\Delta H_c|}{\Delta H_f (1 - w_f)} \times 100\%; \quad (1 - w_f) = w_m, \quad (4)$$

where:  $\Delta H_m$  and  $\Delta H_c$  are values of the melting enthalpy and the cold crystallization enthalpy, respectively ( $\Delta H_m$  is positive and  $\Delta H_c$  is negative).

The value for  $\Delta H_f$  represents the melting enthalpy of PPS at 100 % crystallinity (or PEEK with 100 % crystallinity); these values are 150.4 J/g for PPS and 130 J/g for PEEK, respectively [18, 19]. The matrix weight fraction ( $w_m = 1 - w_f$  calculated from Eq. 4 for LAMP1, LAMP2 and LAMP3 is provided by the manufacturers and equals to 0.34 for both, the tape and the laminate (this value (0.34) is used for calculations).

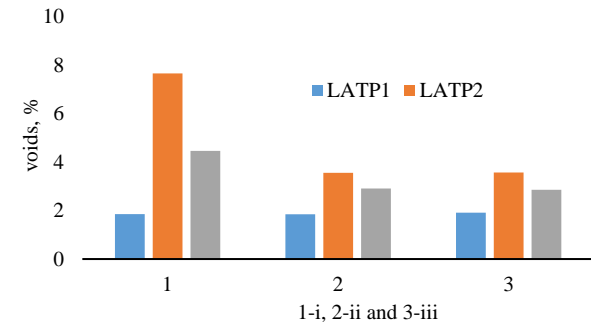
## 3. RESULTS AND DISCUSSION

### 3.1. Void content in laminates

Fig. 3 d presents various locations within the tested composite samples, where void content were measured by optical microscopy. Void content is increased during the LAMP2 process while it is reduced in the case of LAMP3. This is an important observation and indicates that void rebound has occurred during the LAMP process.

Void content in the composite was determined according to two methods: 10 images (first method) and 10 samples (for second method) [39, 40]. In the LAMP1 sample voids are up to 2 %, while in the LAMP2 sample, voids are noted with max value of 8.7 %. For LAMP3 samples, the max value of void content reached to ~ 6.3 %. The void content is relatively higher for LAMP2 and LAMP3, but still they belong within the allowed average limits for thermoplastic that usually is up to 5+/-1 %). For samples of LAMP2, void content is relatively high and required further experimentation to overcome this issue in order to manufacture a composite within allowed void content and acceptable mechanical properties. Fig. 3 2D microscopy images from a cross-section of samples LAMP 1-3: (i)

sample extracted at the beginning of LAMP process (process has just started); (ii) sample extracted from the mid region (the process is in its middle regime); (iii) sample extracted from the region at the final stage of LAMP process.



Type	i	i	ii	iii	iii	Average
LAMP1	1.90	1.80	1.80	1.87	1.87	1.87
	1.78	1.92	1.89	2.05	1.86	
LAMP2	8.77	7.32	3.65	2.36	2.78	5.19
	6.73	7.76	3.45	5.65	3.45	
LAMP3	6.29	3.22	2.56	2.23	0.96	3.50
	5.43	2.87	3.24	4.23	3.98	

Fig. 2. Calculation of average voids with optical microscopy for samples LAMP1-3 in different regions: i, ii and iii

Void content is higher at the beginning of the LAMP process (i) while it is reduced towards the mid and the end

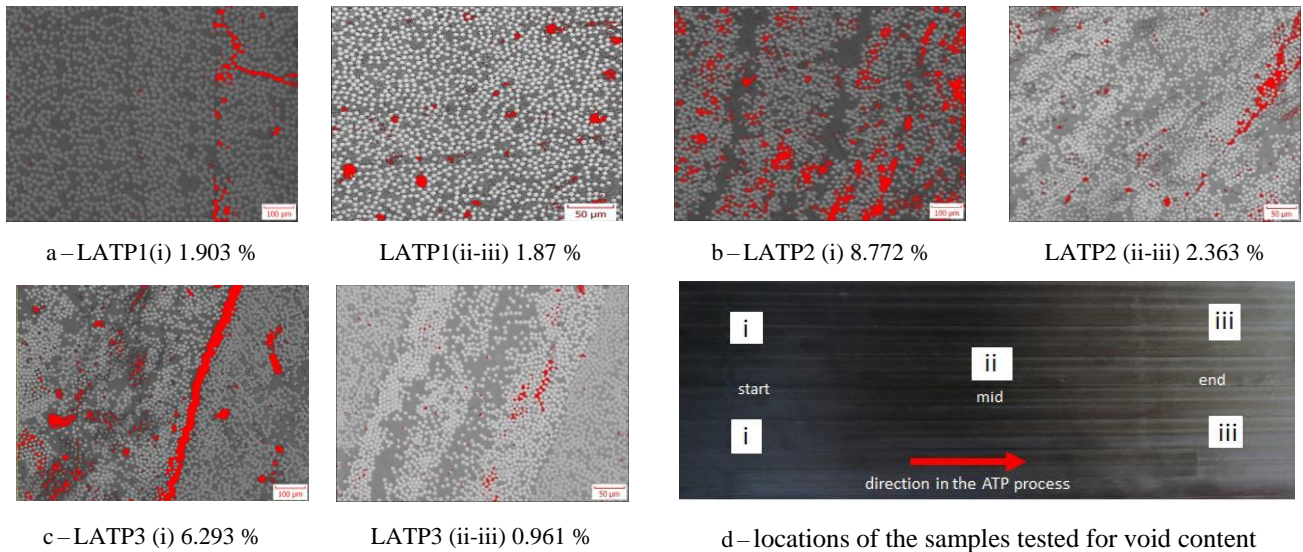


Fig. 3. Images taken by optical microscopy for LAMP1-3 samples and void distribution calculated with software ImageJ (in %). The images show max and min void content as well as distribution of phases (polymer matrix and voids) in two different spots (i and ii-iii) on cross section of LAMP 1-3 samples

Table 3. Comparison of flexural properties of autoclave and ATP manufactured composites

Material	Autoclave strength, MPa	ATP Heat source	Lay-down speed, m/min	Strength average, MPa	Translation
AS4/PEEK [37]	1500	Hot Gas Torch	1.8	> 1500	100 %
CF*/PEEK [34]	1650	/	/	/	/
IM7/PEEK [27]	1775	Laser	8	1207	70 %
AS4/PEEK LAMP2	1650	Laser	9	1143	69.2 %
AS4/PPS LAMP1	1650	Laser	9	1167	70.7 %
AS4/PPS/PEEK LAMP3	1650	Laser	9	1035	62 %

\*Fibre type not further specified.

region of the plate during LAMP process (ii and iii, respectively) Fig. 2. This phenomenon is due to the high power of the laser at the beginning of the LAMP process. In the following experimental tests [42] with less laser power there is a reduced void contents at the beginning of the LAMP process, and actually there is no big difference in the void contents all through the sample length or thickness.

### 3.2. Mechanical tests of laminates

The results of mechanical tests performed on materials manufactured by LAMP process for three tested samples are presented in this section. Overall, the material produced by LAMP1 performed better properties compared to reference data of the autoclaved material [27] in terms of flexural strength and flexural stiffness. These data are summarized in Table 3.

The significant knockdown in flexural strength for the LAMP process (compared to autoclaved samples, Table 3) is thought to be a consequence of morphology and void rebound as discussed previously in section 3.1.

### 3.3. Degree of crystallinity of laminates

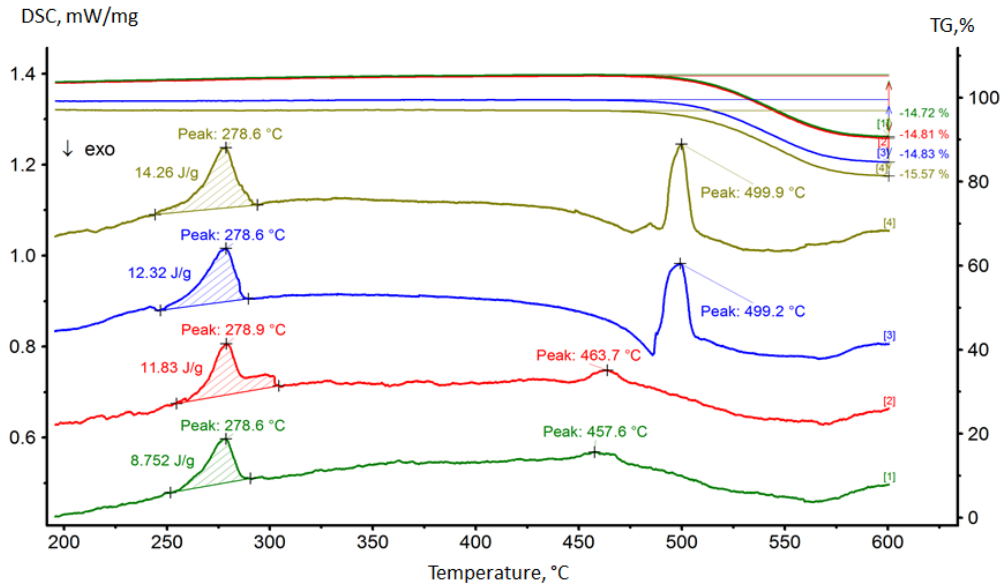
Fig. 4–Fig. 6 present DSC diagrams for specimens LAMP1, LAMP2 and LAMP3, respectively. These specimens were tested at room temperature and later annealed (thermally treated) at 75, 100 and 150 °C for 60 minutes, and then examined again on DSC under the same conditions.

The DSC traces of these specimens LAMP1 (UD carbon-PPS tape, Fig. 4) does not show the exothermal cold crystallization peak. These specimens were fully crystallized during the annealing step, a degree of crystallinity ranges from 17.1 to 27.9 %.

A DSC analysis also confirmed that the laminate reached maximum crystallinity with a value of  $X_c = 27.9\%$ . The carbon-PPS samples start to decompose when temperature reaches about 500 °C.

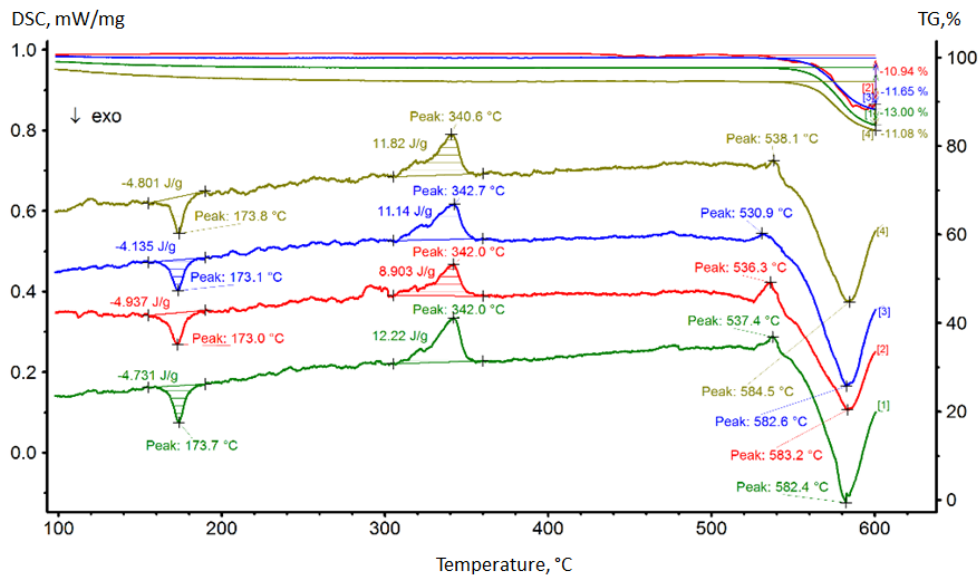
Fig. 5. shows the DSC heating traces of the LAMP2 (UD carbon-PEEK tape). The laminate LAMP2 shows a cold crystallization peak at 173 °C.

Fig 6 shows the DSC heating traces of the LAMP3 (UD carbon-PEEK/PPS tape). The laminate LAMP3 shows a cold crystallization peak at 173 °C and a melt peak at 342 °C for PEEK matrix as well as a melt peak at 278 °C for PPS matrix. The DSC traces of these specimens do not show the exothermal cold crystallization peak for PPS matrix. The decomposition process starts at temperatures of  $\approx 480$  °C.



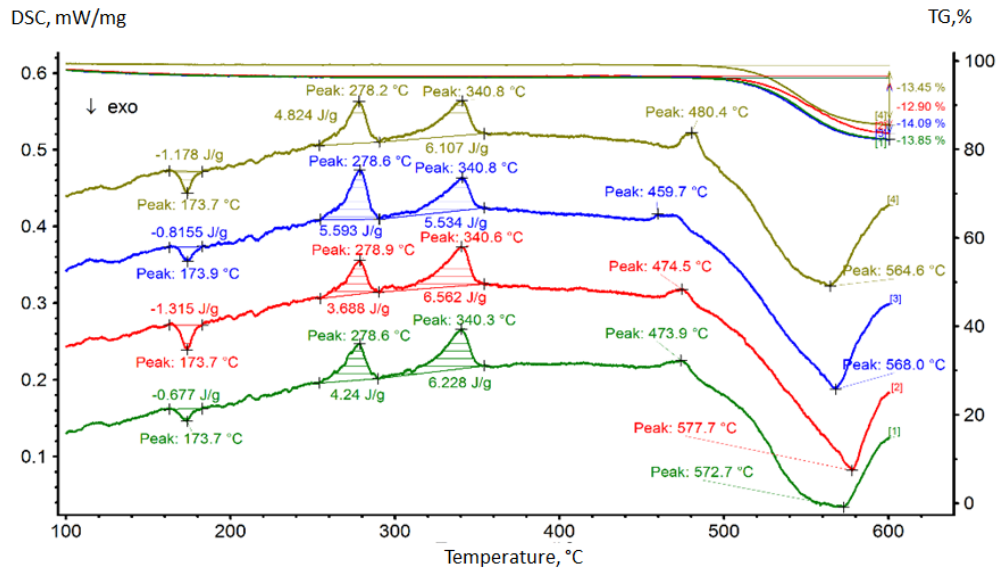
File	Sample	Range	Atmosphere
DSC-TG-PPS-CF RT sample LAMP1	PPS-CF-RT	27.0/10.0(K/min)/600.0	ARGON/60/no gas/ARGON/10
DSC-TG-PPS-CF 75°C-1h sample LAMP1	PPS-CF-75°C-1h	27.0/10.0(K/min)/600.0	ARGON/60/no gas/ARGON/10
DSC-TG-PPS-CF 100°C-1h sample LAMP1	PPS-CF-100°C-1h	27.0/10.0(K/min)/600.0	ARGON/60/no gas/ARGON/10
DSC-TG-PPS-CF 150°C-1h sample LAMP1	PPS-CF-150°C-1h	27.0/10.0(K/min)/600.0	ARGON/60/no gas/ARGON/10

Fig. 4. DSC/TGA curves from LAMP1 of the as-received tape and the welded tapes, before and after an annealing steps



File	Sample	Range	Atmosphere
DSC-TG-PEEK-CF RT sample LAMP2	PEEK-CF-RT	27.0/10.0(K/min)/600.0	ARGON/60//ARGON/10
DSC-TG-PEEK-CF 75°C-1h sample LAMP2	PEEK-CF-75°C-1h	27.0/10.0(K/min)/600.0	ARGON/60//ARGON/10
DSC-TG-PEEK-CF 100°C-1h sample LAMP2	PEEK-CF-100°C-1h	27.0/10.0(K/min)/600.0	ARGON/60//ARGON/10
DSC-TG-PEEK-CF 150°C-1h sample LAMP2	PEEK-CF-150°C-1h	27.0/10.0(K/min)/600.0	ARGON/60//ARGON/10

Fig. 5. DSC/TGA curves for LAMP2 of the as-received tape and the welded tapes, before and after an annealing steps



File	Sample	Range	Atmosphere
DSC-TG-PPS/PEEK-CF RT sample LAMP3	PPS/PEEK-CF-RT	27.0/10.0(K/min)/600.0	ARGON/60/ARGO/10
DSC-TG-PPS/PEEK-CF 75°C-1h sample LAMP3	PPS/PEEK-CF-75°C-1h	27.0/10.0(K/min)/600.0	ARGON/60/ARGO/10
DSC-TG-PPS/PEEK-CF 100°C-1h sample LAMP3	PPS/PEEK-CF-100°C-1h	27.0/10.0(K/min)/600.0	ARGON/60/ARGO/10
DSC-TG-PPS/PEEK-CF 150°C-1h sample LAMP3	PPS/PEEK-CF-150°C-1h	27.0/10.0(K/min)/600.0	ARGON/60/ARGO/10

**Fig. 6.** DSC/TGA curves for LAMP3 of the as-received tape and the welded tapes, before and after an annealing steps

In Table 4 are presented values of degree of crystallinity ( $X_c$ ) calculated from DSC diagrams for all examined specimens: LAMP1, LAMP2 and LAMP3.

Fig. 7 presents the degree of crystallinity vs. different temperatures of annealed composites designated as LAMP1, LAMP2 and LAMP3. DSC analysis of LAMP2 manufactured specimens (Fig. 5) revealed 16.9 % crystallization of the PEEK matrix. This is a lower % of crystallinity than the level considered optimal for good mechanical properties (~ 35 %) and optimal chemical resistance. In contrast, the crystallinity of representative autoclaved samples was reported as 40 % by Comer et. al. [27]. The decomposition of carbon-PEEK samples starts at temperatures higher than 530 °C and it is related to exothermic DSC peak (at  $\approx$  580 °C).

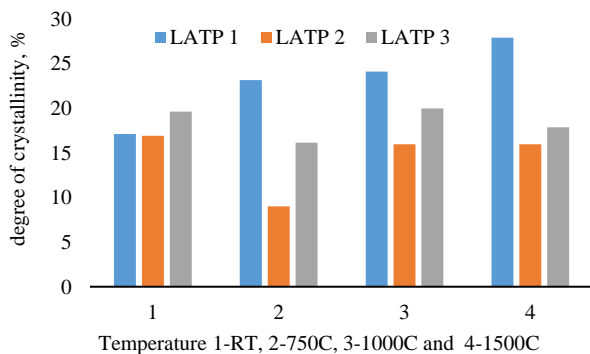


**Fig. 7.** Degree of crystallinity of laminates LAMP1, LAMP2 and LAMP3 annealed at different temperatures, 1 is room temperature 22 °C, 2 refers to 75 °C, 3 refers to 100 °C and 4 is 150 °C

There are two possibility for lower crystallinity of LAMP 1 and LAMP 2 at room temperature (samples are welded tapes before an annealing step):

- First possible reason: during a two-stage pass of the head over the composite material, the bottom side is melted and later during second pass only the top surface is melted. The temperature distribution is not very good through the ply for the very short time of passing the roller over the composite material, namely the heat energy does not reach through the whole thickness of the composite sample.
- The second reason could be that the high cooling rate performed on this sample. The same findings are reported by other authors as well [21].

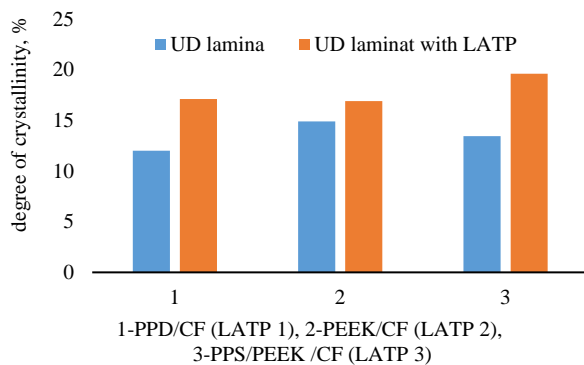
Fig. 8 presents the degree of crystallinity vs. lamina (UD tape from starting) and laminate (final samples with LAMP technology) of composites designated as LAMP1, LAMP2 and LAMP3.

On the other hand, high cooling rates are desirable from the point of view to avoid void rebound once pressure from the roller is released. This study is still in progress; however, the variation and dependence of tool temperature and roller temperature are very important and need to be optimized in further study in order to manufacture composites with optimal mechanical properties.

Table 4 shows the crystallinity degree ( $X_c$ ) of PEEK/CF and PPS/CF. According to data presented in Table 4, the  $X_c$  of pure PEEK/CF (LAMP 2) and pure PPS/CF (LAMP1) can be calculated to 16.94 % and 17.13 %, respectively, for studies at room temperature.

**Table 4.** Degree of crystallinity ( $X_c$ ) of LAMP 1, LAMP2 and LAMP3 composite materials

		$\Delta H_m$ J/g PPS	$\Delta H_m$ J/g PEEK	$\Delta H_c$ PEEK J/g	$\Delta H_f$ J/g	Degree of cryst. %		
						PPS	PEEK	PPS/PEEK
LAMP 1 (PPS/CF)	RT	8.75	/	/	51.1	17.13	/	/
	75	11.83	/	/	51.1	23.15	/	/
	100	12.32	/	/	51.1	24.11	/	/
	150	14.26	/	/	51.1	27.97	/	/
LAMP 2 (PEEK/CF)	RT	/	12.22	4.73	44.2	/	16.94	/
	75	/	8.030	4.94	44.2	/	7.00	/
	100	/	11.14	4.14	44.2	/	15.85	/
	150	/	11.82	4.80	44.2	/	15.88	/
LAMP 3 (PPS/PEEK/CF)	RT	4.23	6.04	0.94	47.6	19.96	19.15	19.61
	75	3.62	5.89	1.83	47.6	15.90	16.38	16.14
	100	5.64	4.93	1.06	47.6	15.16	25.50	19.97
	150	4.63	5.27	1.40	47.6	15.15	20.93	17.85

**Fig. 8.** Degree of crystallinities of laminates LAMP 1-3 annealed at different temperatures

From data presented in this study, it could be concluded that LAMP 1 sample (PPS/CF) showed an increase in the degree of crystallinity with increasing of annealing temperature from 17.1 % (at room temperature) to 27.9 % (at 150 °C). No induced crystallization was observed here before the annealing temperature that shows that the amount of material that could be affected by slow heating has already crystallized during the annealing step.

For results obtained from samples LAMP2 and LAMP3, the degree of crystallinity is reduced. It was observed that heating the composite material to a certain temperature followed by gradual cooling down in oven, subsequent will cause a small exothermic peak that shows that the amount of material has not already crystallized during the annealing. The induced crystallization probably takes place continuously between the glass transition and the melting temperature for the PEEK matrix which is higher than 150 °C.

Compared to pure PEEK/CF (LAMP2), the  $X_c$  of PEEK in binary alloys (LAMP3) increased when PPS was added. The  $X_c$  of PPS in PEEK/PPS alloys decreases when PEEK increases for increase of temperature (for LAMP 3 presented in Table 4 at room temperature and 150 °C). The crystallinity degree of PEEK is improved when PPS/CF was added.

#### 4. CONCLUSIONS

This study covers Laser assisted tape placement process of manufacturing of three types of samples based on

LAMP1, LAMP2 and LAMP3 laminates. The work of tested samples LAMP 1-3 could be summarized as follows:

1. During the heating step between the glass transition and the melting point, partial melting and recrystallization take place in observed samples which result in a higher degree of perfection in the crystalline regions (LAMP1 samples), higher crystallinity.
2. Flexural strength in this study is ~ 70 % of the flexural strength that is measured with autoclave process. These values are similar with those ones that are already reported in literature (given in Table 3). The void % is higher for the last two samples, that means it affects the flexural strength of the samples.
3. In PEEK matrix samples (LAMP2 and LAMP3) there is a peak of enthalpy of crystallization at all aging temperatures; the aging occurs at temperatures lower than the glass temperature for the PEEK matrix.
4. Since the glass transition temperatures of thermoplastic matrices are: ~ 155 °C for PEEK and 85 °C for PPS, it is already in author's plan to continue the aging of these composites at higher temperatures and consequently examination of the degree of crystallinity of those annealed composite laminates.
5. Void contents are within the allowed void tolerance for thermoplastic such as for LAMP1; however, in further studies targets are focused to manufacture of composite materials by ATP with-less voids contents and better consolidated laminates.

#### Acknowledgments

The authors would like to acknowledge the support of the research team from Institute for advanced composites and robotics- Prilep and engineering team from Mikrosam A.D. –Prilep (R.Macedonia).

#### REFERENCES

1. **Dubé, M.** Static and Fatigue Behaviour of Thermoplastic Composite Laminates Joined by Resistance Welding, *PHD Thesis*, McGill University Montreal, Canada, 2007: pp. 63–94.
2. **Brecher, C., Emonts, M., Schares, R.L., Stimpfl, J.** CO<sub>2</sub>-Laser-assisted Processing of Glass Fiber-reinforced Thermoplastic Composites *Proceedings of SPIE* 8603, 2013: pp. 86030H. <https://doi.org/10.1117/12.1000243>.

3. **Fink, B.K., Gillespie, J.W., Ersoy, N.B.** Thermal Degradation Effects on Consolidation and Bonding in the Thermoplastic Fiber-Placement Process, Army research laboratory, 2000: pp. 10–29.
4. **Maurer, D., Mitschang, P.** Laser-powered Tape Placement Process – simulation and Optimization *Journal Polymer & Composites Science* 1 (3) 2015: pp. 129–137. <https://doi.org/10.1080/20550340.1114798>
5. **Reichardt, J., Baran, I., Akkerman, R.** New Analytical and Numerical Optical Model for the Laser Assisted Tape Winding Process *Composites Part A* 107 2018: pp. 647–656. <https://doi.org/10.1016/j.compositesa.2018.01.029>
6. **Bandaru, A.K., Clancy, G., Peters, D., Ronan O' Higgins, R., Weaver, P.M.** Interface Characterization of Thermoplastic Skin- Stiffener Composite Manufactured using Laser-Assisted Tape Placement *AIAA/ASCE/AHS/ASC Structures, Structural Dynamics and Materials Conference* 2018 <https://doi.org/10.2514/6.2018-0481>
7. **Clancy, G.J., Peeters, D., Oliveri, V., Jones, D., O'Higgins, R., Weaver, P.M.,** Steering of Carbon Fiber/Thermoplastic Pre-preg Tapes using Laser-Assisted Tape Placement *AIAA/ASCE/AHS/ASC Structures, Structural Dynamics, and Materials Conference* 8-12 Jan. Kissimmee, Florida 2018 <https://doi.org/10.2514/6.2018-0478>
8. **Clancy, G., Peeters, D., Oliveri, V., Jones, D., O'Higgins, R.M., Weaver, P.M.** A Study of the Influence of Processing Parameters on Steering of Carbon Fibre/PEEK Tapes using Laser-Assisted Tape Placement *Composites Part B* 2018: pp. 243–251. <https://doi.org/10.1016/j.compositesb.2018.11.033>
9. **Di Francesco, M., Giddings, P.F., Scott, M., Goodman, E., Dell' Anno, G., Potter, K.** Influence of Laser Power Density on the Meso Structure of Thermoplastic Composite Preforms Manufactured by Automated Fibre Placement *In International SAMPE Technical Conference Journal of Advanced Materials* (3) 2016: pp. 141–155.
10. **Stokes-Griffin, C.M., Compston, P., Matuszyk, T.I., Cardew-Hall, M.J.** Thermal Modelling of the Laser-assisted Thermoplastic Tape Placement Process *Journal of Thermoplastic Composite Materials* 28 (10) 2013: pp. 1445–1462. <https://doi.org/10.1177/0892705713513285>
11. **Stokes-Griffin, C.M., Compston, P.,** Laser-Assisted Tape Placement of Thermoplastic Composites: The Effect of Process Parameters on Bond Strength *Sustainable Automotive Technologies* 2014: pp. 133–141. [https://doi.org/10.1007/978-3-319-01884-3\\_13](https://doi.org/10.1007/978-3-319-01884-3_13)
12. **Cornelis, H., Kander, R.G., Martin, J.P.** Solvent-induced Crystallization of Amorphous Poly (ether ether ketone) by Acetone *Polymer* 37 (20) 1996: pp. 4573–4578. [https://doi.org/10.1016/0032-3861\(96\)00246-7](https://doi.org/10.1016/0032-3861(96)00246-7)
13. **Blundell, D.J., Osborn, B.N.** The Morphology of Poly (Aryl-Ether-Ether- Ketone) *Polymer* 24 (8) 1983: pp. 953–958. [https://doi.org/10.1016/0032-3861\(83\)90144-1](https://doi.org/10.1016/0032-3861(83)90144-1)
14. **Muzzy, J.D., Bright, D.G., Hoyos, G.H.** Solidification of Poly (Ethylene Terephthalate) with Incomplete Crystallization *Polymer Engineering and Science* 18 (6) 1978: pp. 437–442. <https://doi.org/10.1002/pen.760180604>
15. **Unger, W.J., Hanse, J.S.** The Effect of Thermal Processing on Residual Strain Development in Unidirectional Graphite Fibre Reinforced PEEK *Journal of Composite Materials* 27 (1) 1993: pp. 59–82. [https://doi.org/10.1002/0021-9983\(199301\)27:01<59::AID-JCOM27010059-24>3.0.CO;2-1](https://doi.org/10.1002/0021-9983(199301)27:01<59::AID-JCOM27010059-24>3.0.CO;2-1)
16. **Tierney, J.J., Gillespie, Jr.J.W.** Crystallization Kinetics Behavior of PEEK Based Composites Exposed to High Heating and Cooling Rates *Composites Part A* 35 (5) 2004: pp. 547–558. <https://doi.org/10.1016/j.compositesa.2003.12.004>
17. **Risteska, S., Samak, S., Sokolowski, Z., Bogdanoski, D.** Integrated Production Solutions for Thermoplastic Materials *6-th International Scientific Conference Space Technologies* 2017: pp. 158.
18. **Risteska, S., Samak, S., Sokolowski, Z., Bogdanoski, D.** Solutions for Production and Properties of Thermoplastic Composites *The 10<sup>th</sup> Asian-Australasian Conference* 16-19 October, 2016: M28-2.
19. **Hoang, M.D.** Procedure for Making Flat Thermoplastic Composite Plates by Automated Fiber Placement and Their Mechanical Properties, MSs Thesis Concordia University Montreal, Quebec, Canada, 2015.
20. **Talbott, M.F., Springer, G.S., Berglund, L.A.** The Effects of Crystallinity on the Mechanical Properties of PEEK Polymer and Graphite Fiber Reinforced PEEK *Journal of Composite Materials* 21 (11) 1987: pp. 1056–1087. <https://doi.org/10.1177/002199838702101104>
21. **Sonmez, F.Z., Hahn, H.T.** Modeling of Heat Transfer and Crystallization in Thermoplastic Composite Tape Placement Process *Journal of Thermoplastic Composite Materials* 10 (3) 1997: pp. 198–240. <https://doi.org/10.1177/089270579701000301>
22. **Xu, H., Hu, J.** Study of Polymer Matrix Degradation Behavior in CFRP Short Pulsed Laser Processing *Polymers* (8) 2016: pp. 299–313. <https://doi.org/10.3390/polym8080299>
23. **Comer, A., Hhammond, P., Ray, D., Lyons, J., Obande, W., Jones, D., O'Higgins, R., McCarthy, M.** Wedge Peel Interlaminar Toughness of Carbon-fibre/peek Thermoplastic Laminates Manufactured by Laser-assisted Automated-Tape-Placement (LATP) *Conference: SETEC 2014 Tampere Conference&Table Top Exhibition* 2014: pp. 51–119. <https://doi.org/10.13140/2.1.1305.9847>
24. **Kuo, M.C., Tsai, C.M., Huang, J.C., Chen, M.** PEEK Composites Reinforced by Nano-sized SiO<sub>2</sub> and Al<sub>2</sub> O<sub>3</sub> Particulates *Materials Chemistry and Physics* 90 2005: pp. 185–195. <https://doi.org/10.1016/j.matchemphys.2004.10.009>
25. **Spruiell, J.E., Janke, C.J.** A Review of the Measurement and Development of Crystallinity and its Relation to Properties in Neat Poly (Phenylene Sulfide) and its Fber Reinforced Composites, *Technical Report*, Oak Ridge National Laboratory, 2004.
26. **Herrod-Taylor, A.** The Crystallization of Poly (Aryl Ether Ether Ketone) (PEEK) and its Carbon Fibre Composites, *MSc Thesis*, University of Birmingham, United Kingdom, 2011.
27. **Comer, A.J., Ray, D., Obande, W.O., Jones, D., Lyons, J., Rosca, I., O'Higgins, R.M., McCarthy, M.A.** Mechanical Characterization of Carbon Fibre–PEEK Manufactured by Laser-assisted Automated-Tape-Placement and Autoclave Composites (*Applied Science and Manufacturing*): Part A 69 2015: pp. 10–20. <https://doi.org/10.1016/j.compositesa.2014.10.003>
28. **Gao, S.L., Kim, J.K.** Cooling Rate Influences in Carbon Fbre/PEEK Composites *Composites Part A: Applied Science and Manufacturing* 31 (6) 2000: pp. 517–530.



- [https://doi.org/10.1016/S1359-835X\(00\)00009-9](https://doi.org/10.1016/S1359-835X(00)00009-9)
29. **Grouve, W.** Weld Strength of Laser-assisted Tape-Placed Thermoplastic Composites, *PhD Thesis*, University of Twente, Enschede, The Netherlands, 2012.
  30. **Cai, X.** Determination of Process Parameters for the Manufacturing of Thermoplastic Composite Cones Using Automated Fiber Placement, *MSc Thesis*, Concordia University Montreal, Quebec, Canada, 2012.
  31. **De Jesus Silva, A.J., Berry, N.G., da Costa, M.F.** Structural and Thermo-mechanical Evaluation of Two Engineering Thermoplastic Polymers in Contact with Ethanol Fuel from Sugarcane *Materials Research* 19 (1) 2016: pp. 84–97.  
<https://doi.org/10.1590/1980-5373-MR-2015-0480>.
  32. **Kilroy, J.P., Ó'Brádaigh, C., Semprimoschnig, C.O.** Mechanical and Physical Evaluation of a New Carbon Fbre/PEEK Composite System for Space Applications *SAMPE Journal* 44 (3) 2008: pp. 22–34.
  33. **Lamontia, M.A., Gruber, M.B., Tierney, J.J., Gillespie, Jr.J.W., Jensen, B.J., Cano, R.J.** Modelling the Accudyne Thermoplastic in Situ ATP process *In: Proceedings of SAMPE conference 23-24 March, 2009*.
  34. **Cano, R.J., Belvin, H.L., Hulcher, A.B., Grenoble, R.W.** Studies on Automated Manufacturing of High-Performance Composites *Presented at the American Helicopter Society Hampton Roads Chapter, Structure Specialists' Meeting*, Williamsburg, Virginia, USA, October 30–1 November 2001.
  35. [http://welshcomposites.co.uk/downloads/Microscopy%20W ebinar.pdf](http://welshcomposites.co.uk/downloads/Microscopy%20W%20ebinar.pdf)
  36. **Hayes, B.S., Gammon, L.M.** Optical Microscopy of Fiber-Reinforced Composites – Chapter 1: Introduction Composite Materials and Optical Microscopy, ASM International, Materials Park, Ohio 44073-0002, 2010.  
[www.asminternational.org](http://www.asminternational.org)
  37. **Paciornik, S., D'Almeida, J.R.M.** Measurement of Void Content and Distribution in Composite Materials through Digital Microscopy *Journal of Composite Materials* 43 (2) 2009: pp 101–112.  
<https://doi.org/10.1177/0021998308098234>
  38. Image J program developed at the National Institutes of Health (NIH)  
<https://en.wikipedia.org/wiki/ImageJ>
  39. **ASTM D 3171.** Standard Test Methods for Constituent Content of Composite Materials.
  40. **ASTM D 792.** Standard Test Methods for Density and Specific Gravity (Relative Density) of Plastics by Displacement.
  41. **EN ISO 14125.** Fibre-reinforced Plastic Composites Determination of Flexural Properties English version of DIN EN ISO 14125 (ISO 14125: 1998).
  42. **Samak, S., Sokoloski, Z., Risteska, S., Bogdanoski, D.** Improving the Final Properties of Thermoplastic Composites Manufactured with Laser Automated Tape Placement (LATP) *The 13<sup>th</sup> SAMPE CHINA Conference & Exhibition 16-18 May, 2018*.